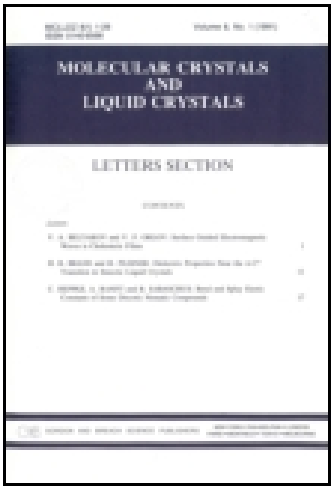

Molecular Crystals and Liquid Crystals
Publication details, including instructions for authors and subscription information:
http://www.tandfonline.com/loi/gmcl20

Spectroscopic Study and Quantum Chemical Analysis of the Asymmetrical Cationic Polymethine Dye Versus Its Symmetrical Analogues

N. V. Bashmakova [a b], Ye. O. Shaydyuk [a], O. V. Przhonska [a], G. V. Klishevich [a], V. I. Melnyk [a], O. D. Kachkovsky [c], Yu. L. Slominsky [c] & M. V. Bondar [a]

[a] Institute of Physics, Prospect Nauki, 46, Kyiv-28, 03028, Ukraine

[b] Taras Shevchenko National University of Kyiv, Volodymyrska Street, 60, Kyiv, 01601, Ukraine

[c] Insitute of Organic Chemistry, Murmanskaya Street, 5, Kyiv, 03094, Ukraine

Published online: 28 Mar 2014.

To cite this article: N. V. Bashmakova, Ye. O. Shaydyuk, O. V. Przhonska, G. V. Klishevich, V. I. Melnyk, O. D. Kachkovsky, Yu. L. Slominsky & M. V. Bondar (2014) Spectroscopic Study and Quantum Chemical Analysis of the Asymmetrical Cationic Polymethine Dye Versus Its Symmetrical Analogues, Molecular Crystals and Liquid Crystals, 590:1, 199-212, DOI: 10.1080/15421406.2013.874729

To link to this article: http://dx.doi.org/10.1080/15421406.2013.874729

Mol. Cryst. Liq. Cryst., Vol. 590: pp. 199–212, 2014

ISSN: 1542-1406 print/1563-5287 online
DOI: 10.1080/15421406.2013.874729

Spectroscopic Study and Quantum Chemical Analysis of the Asymmetrical Cationic Polymethine Dye Versus Its Symmetrical Analogues

N. V. BASHMAKOVA,[1,2,*] YE. O. SHAYDYUK,[1]
O. V. PRZHONSKA,[1] G. V. KLISHEVICH,[1] V. I. MELNYK,[1]
O. D. KACHKOVSKY,[3] YU. L. SLOMINSKY,[3]
AND M. V. BONDAR[1]

[1]Institute of Physics, Prospect Nauki, 46, Kyiv-28, 03028, Ukraine
[2]Taras Shevchenko National University of Kyiv, Volodymyrska Street, 60, Kyiv, 01601, Ukraine
[3]Insitute of Organic Chemistry, Murmanskaya Street, 5, Kyiv, 03094, Ukraine

A detailed investigation of the steady-state and time-resolved spectral properties of new cationic asymmetrical trimethine cyanine dye with indolenine and benzoimidazole terminal groups has been performed in comparison with its symmetrical analogues. Steady-state measurements included absorption, fluorescence, excitation anisotropy in several solvents of different polarity and viscosity. Kerr-gated time-resolved study of the fluorescence properties has been performed using 1κHz femtosecond laser system. Experimental results are in agreement with DFT/6-31(d,p)/B3LYP quantum chemical calculations, allowing determination of the charge distribution, bond length alternation, permanent and transition dipole moments, energy levels and the leading molecular orbital configurations responsible for the lowest electronic transitions.

Keywords Polymethine dye; time-resolved spectroscopy; quantum chemical analysis.

Introduction

Polymethine dyes (PDs) represent a large class of organic molecules with the absorption bands covering a broad spectral range from ≈400 nm up to near IR region ≈1600 nm, broader than any other class of dyes. Their molecular structures typically contain π-conjugated chromophore with the odd number of carbon atoms (or polymethine chain) and electron-donor (D) or electron-acceptor (A) terminal groups forming the following basic arrangements: D–π–D, A–π–A or D–π–A. If the terminal groups are of the same chemical constitution, PDs are called symmetrical and belong to C_{2V} symmetry group. If the terminal groups differ in their molecular structures, PDs are called asymmetrical. PDs have been known for more than a century and extensively studied due to their numerous applications as fluorescent probes in chemistry and biology, active and passive laser media, photosensitizers in photography, materials for memory devices, photodynamic therapy, electroluminescence, etc. [1–2]. Large molar absorbance of PDs (up to 3×10^5 $M^{-1}cm^{-1}$) and possibility to tune

*Address correspondence to N. V. Bashmakova. E-mail: n.bashmakova@gmail.com

their absorption bands from the visible to near IR region via specific structural modifications are key factors for the development of PD-based organic materials for nonlinear optical applications including all-optical signal processing [3–4]. Many aspects of the optical and electronic properties of PDs are already well understood; see for example reviews [1–2, 5–6 and references therein].

In this study, a new asymmetrical polymethine dye consisting of two terminal groups with strongly different donor properties, D'–π–D, have been synthesized and investigated with the goal of obtaining a detailed description of its linear optical properties in comparison with the symmetrical analogues: D–π–D and D'–π–D'. Here we present a detailed report on the photophysical properties of this new compound. We describe: (1) synthesis of D'–π–D molecule; (2) linear absorption, fluorescence, and quantum yield of D'–π–D, as well as its symmetrical analogues, in several solvents of the different polarity and viscosity, (3) excitation anisotropy spectra; (4) fluorescence lifetimes and decay kinetics measured by time-resolved Kerr-gated method using femtosecond laser system; (5) comparison of the spectroscopic properties of D'–π–D molecule with its symmetrical analogues; and (6) detailed quantum-chemical analysis providing insight into the nature of the linear properties of the investigated compounds. The combination of the experimental methods and their theoretical analysis gave us information about the energy-level structures in agreement with the observed optical processes.

Experimental

The molecular structures of PDs studied in this paper are shown in Fig. 1. Their chemical names are the following: D–π–D compound: 1,3,3-trimethyl-2-(3-(1,3,3-trimethylindolin-2-ylidene)prop-1-en-1-yl)-3H-indol-1-ium tetrafluoroborate (Astraphloxin), (labeled as PD AF); D'–π–D' compound: 5-(benzo[d]oxazol-2-yl)-2-(3-(5-(benzo[d]oxazol-2-yl)-3-ethyl-1-phenyl-1H-benzo[d]imidazol-2(3H)-ylidene)prop-1-en-1-yl)-3-ethyl-1-phenyl-1H-benzo[d]imidazol-3-ium tetrafluoroborate, labeled as PD 3338 and D'–π–D compound: 5-(benzo[d]oxazol-2-yl)-3-ethyl-1-phenyl-2-(3-(1,3,3-trimethylindolin-2-ylidene)prop-1-en-1-yl)-1H-benzo[d]imidazol-3-ium tetrafluoroborate, labeled as PD 3294. Symmetrical cationic dye PD AF, synthesized by the standard method [7], is known since the 50th of the last century and is well-characterized photophysically. Its nonlinear optical properties, including two-photon absorption spectra, have been also investigated [8]. Symmetrical cationic PD 3338 has been synthesized using procedure described earlier [9]. 1H-NMR (DMSO-d6), δ (ppm): 1.29 (t, J = 6.0 Hz, 6H), 4.13 (q, J = 6.0, 4H), 5.57 (d, J = 13.6Hz, 2H), 7.01 (d, J = 8.4Hz, 2H), 7.13 (t, J = 13.6Hz, 1H), 7.40-7.50 (m, 8H), 7.62-7.83 (m, 10H), 8.09 (d, J = 8.4Hz, 2H), 8.34 (s, 2H). Anal. calcd. for C47H37BF4N6O2: C, 70.15; H, 4.63; N, 10.44. Found: C, 69.88; H, 4.77; N, 10.20. Note that spectroscopic properties of PD 3338 have not been yet studied. New asymmetrical compound PD 3294 has been synthesized by condensation of 3-ethyl-2-methyl-1-phenyl-5-(benzo[d]oxazol-2-yl)-benzo[d]imidazol-3-ium4-methylbenzenesulfonate with (1,3,3-trimethyl-1,3-dihydro-2H-indol-2-ylidene)ethanal in acetic anhydride with DBN [10]. 1H-NMR (DMSO-d6), δ (ppm): 1.02 (s, 6H), 1.55 (t, J = 7.2 Hz, 3H), 3.32 (s, 3H), 4.68 (q, J = 7.2 Hz, 2H), 5.89 (d, J = 12.3 Hz, 1H), 6.44 (d, J = 15.0 Hz, 1H), 7.00-7.55 (m, 8H), 7.80-8.10 (m, 6H), 8.27 (d, J = 8.7 Hz, 2H), 8.69 (s, 1H). Anal. calcd. for C36H33BF4N4O: C, 69.24; H, 5.33; N, 8.97. Found: C, 69.02; H, 5.16; N, 9.02. All starting materials and solvents were purchased from Aldrich and used without further purification. 1H-NMR spectra were recorded on a Varian GEMINI 2000 (400.07 MHz) spectrometer at 25°C using tetramethylsilane as an internal standard.

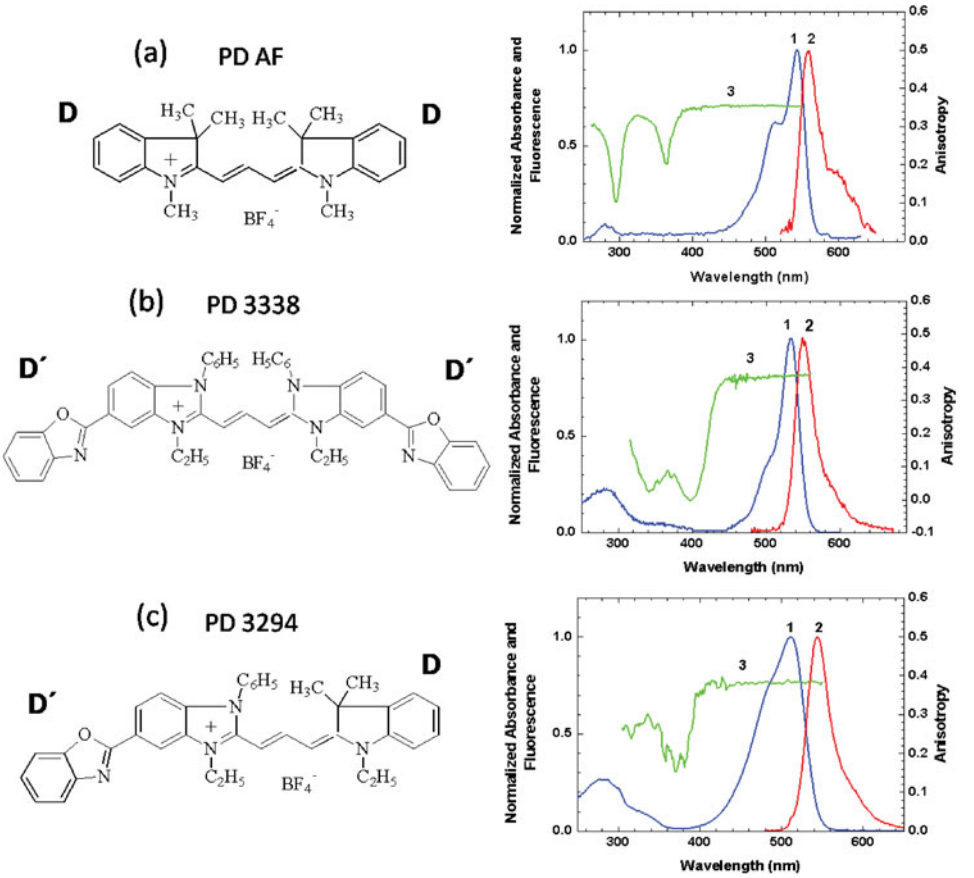

Figure 1. Molecular structures of PD AF (a), PD 3338 (b) and PD 3294 (c), and their normalized absorption (curves 1) and fluorescence (curves 2) spectra in ACN. Excitation anisotropy spectra (curves 3) are measured in glycerol.

The main spectroscopic properties of investigated PDs are determined by the existence of a delocalized π-conjugated system in the polymethine chain and donor terminal groups (identical for symmetrical PDs and different for asymmetrical dye), which themselves possess delocalized π-system and may increase the overall conjugation. The linear absorption spectra are obtained with a Shimadzu 2450 UV−visible spectrophotometer, and the steady-state fluorescence and excitation anisotropy spectra are measured using a CM 2203 spectrofluorimeter (Solar, Belarus) in 10 mm spectrofluorometric quartz cuvettes with small concentrations $\approx$1 μM to avoid aggregation and reabsorption. All fluorescence spectra were corrected for the spectral response of the detection system. Fluorescence quantum yields, Φ_F, are measured by standard method of comparison with the reference solution of Rhodamine 6G in ethanol ($\Phi_F = 0.95$) [11]. Linear spectroscopic measurements are conducted in two solvents of different polarity: dichloromethane (DCM) and acetonitrile (ACN). Their polarities, measured by $\Delta f = (\varepsilon-1)/(2\varepsilon+1)-(n^2-1)/(2n^2+1)$, where ε and n are the solvent dielectric constant and the refractive index, respectively, increase from 0.217 for DCM to 0.306 for ACN [12]. This is the largest Δf we can use, since cationic dyes are poorly soluble in less polar solvents than DCM. To understand the role of solvent viscosity,

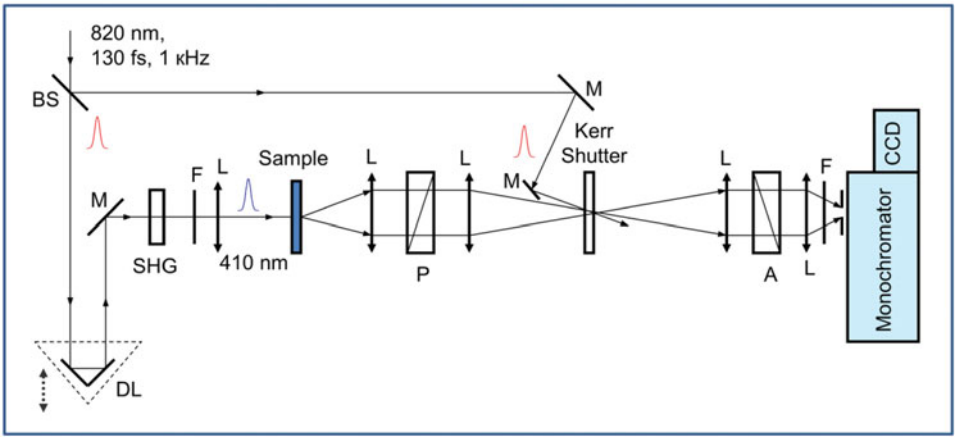

Figure 2. Simplified schematic of the experimental setup: BS - beam splitter; M - 100% reflection mirrors; DL - optical delay line (M-531.DD, PI, Inc.) with retroreflector; SHG - second harmonic generator (BBO crystal); P and A - Glan prisms; F - set of filters; L - focusing lenses; Sample - 1 mm quartz cell with sample solution.

linear spectroscopic measurements were also performed in glycerol (GLY) solutions. All solvents were of spectroscopic grade and used as received.

Fluorescence lifetimes for all dyes are determined by time-resolved Kerr-gated method with the picosecond resolution [13–16]. The experimental setup is shown in Fig. 2, and all decay curves are presented in Fig. 3. The femtosecond laser system is composed by a Ti:Sapphire laser (Mira Optima 900-F), pumped by the second harmonic of CW Nd^{3+}:YAG laser (Verdi-10) and regeneratively amplified by Legent F-1K-HE (all Coherent, Inc.). The output of a laser system was tuned to 820 nm, delivering pulses of 1.6 mJ energy, ≈130 fs (FWHM) with 1 kHz repetition rate. The laser output was divided into two beams. The first beam was converted into the second harmonic, 410 nm, by 1 mm BBO crystal and used as a pump for the sample excitation with ≈2 μJ energy. The second beam (820 nm, ≈250 μJ pulse energy) was utilized as a gate pulse for optical Kerr shutter. As a Kerr-media was used 1 mm glass plate (kron5) with refractive index n = 1,51. The pump and gate pulses were delayed relative to each other by an optical delay line M-531.DD (PI, Inc.). The fluorescence from the samples was collected under magic-angle conditions, polarized with a Glan prism at 45° with respect to the linear polarization of the gate pulse and focused to a Kerr shutter. Time-gated fluorescence was passing through the Glan analyzer and registered with an Acton SP500i spectrometer and a Spec 10 CCD detector.

Results and Discussion

The linear absorption spectra of all compounds are presented in Fig. 1 with the most significant spectroscopic properties listed in Table 1. As seen, all absorption spectra are composed of intense cyanine-like bands, attributed to their $S_0 \rightarrow S_1$ transitions, and relatively weak bands in the UV region corresponding to transitions to higher excited states $S_0 \rightarrow S_n$. The lowest lying absorption band for asymmetrical PD 3294 exhibits a blue shift of 20–30 nm as compare to symmetrical dyes, with slightly broader bandwidth and the smaller peak extinction coefficient (see Table 1). Increasing solvent polarity from DCM to ACN leads to a

Table 1. Measured and calculated parameters for PD AF, PD 3338 and PD 3294

Parameters	Solvents	PD AF	PD 3338	PD 3294
λ^{max}(abs), nm	ACN	543	534	511
	DCM	551	539	524
	GLY	550	540	523
ε^{max}, $M^{-1}\cdot cm^{-1}$	ACN	138,000	224,200	100,300
	DCM	135,000	234,800	108,700
λ^{max}(fl), nm	ACN	558	550	544
	DCM	564	555	548
	GLY	563	556	550
Φ_F,%	ACN	3.0±0.6	14 ± 3	7 ± 1
	DCM	4.0±0.8	18 ± 3	6 ± 1
	GLY	26 ± 5	43 ± 8	35 ± 7
μ_0, D	vacuum	2.3	5.0	10.8
μ_1, D	vacuum	1.3	2.3	3.0
μ_{01}(c), D	vacuum	10.3	10.3	10.0
μ_{01}(exp), D	ACN	11.0	13.0	11.0
τ_F(c), ps	ACN	90 ± 10	270 ± 20	170 ± 20
τ_F(exp), ps	ACN	100 ± 10	270 ± 30	180 ± 20

Notes. λ^{max}(abs) and λ^{max}(fl) - wavelengths of the absorption and fluorescence peaks; ε^{max} - extinction coefficient in the absorption peak; Φ_F - fluorescence quantum yield; μ_0 and μ_1 – calculated permanent dipole moments of the ground, S_0, and the first excited, S_1, states; μ_{01}(c) – calculated $S_0 \rightarrow S_1$ transition dipole moment; μ_{01}(exp) – experimental $S_0 \rightarrow S_1$ transition dipole moment; τ_F(c) and τ_F(exp) – calculated and experimental fluorescence lifetimes, correspondingly. Solvents: ACN – acetonitrile; DCM – dichloromethane; GLY – glycerol.

blue shift of the main absorption peak of all dyes (5–10 nm) indicating a larger stabilization of their ground states in more polar ACN solvent.

Fluorescence spectra of both symmetric compounds, PD AF and PD 3338, in all solvents reveal close to mirror-symmetric shapes with the small Stokes shift demonstrating that the excited-state geometry is not significantly modified from the ground state geometry upon the excitation. In contrast, the fluorescence shape of the asymmetrical PD 3294 is twice more narrow than the absorption bandwidth and is similar to that of symmetrical PDs (independently of solvent polarity and viscosity), confirming the unpolar character of its first singlet excited state, as was determined earlier for asymmetrical PDs [17]. Absorption in the main bands for symmetrical PDs and all fluorescence spectra show comparatively pronounced vibrational structure related to the skeletal C=C vibrational modes with frequencies of 1200–1300 cm^{-1}.

From spectroscopic measurements, we estimate the fluorescence lifetime, $\tau_F = \Phi_F \tau_N$, where the natural lifetime, τ_N, can be calculated from the Strickler-Berg equation, as: $\frac{1}{\tau_N} = 2.88 \times 10^{-9} n^2 \varepsilon^{max} [\frac{\int F(\nu) d\nu \times \int \frac{\varepsilon(\nu)}{\nu} d\nu}{\int \frac{F(\nu)}{\nu^3} d\nu}$, where $F(\nu)$ and $\varepsilon(\nu)$ are the normalized fluorescence and absorption spectra plotted on the wavenumbers, ν, in cm^{-1}; ε^{max} is the molar absorbance at the absorption peak in $M^{-1}\cdot cm^{-1}$, and n is the refractive index of the solvent [18]. For all compounds this equation gives reasonably good agreement ($\approx$ 20%, see Table 1) of the fluorescence lifetimes calculated and directly measured by time-resolved Kerr-gated method. The values of the $S_0 \rightarrow S_1$ transition dipole moments, μ_{01},

can be calculated from the integrated area under the main absorption band according to: $\mu_{01} = \sqrt{\frac{1500\cdot(hc)^2\cdot\ln(10)}{4\pi^3\cdot N_A\cdot E_{01}} \cdot \varepsilon^{\max} \int \varepsilon(\nu)d\nu}$, where h and c are the Planck's constant and velocity of light in vacuum; N_A is the Avogadro's number; $E_{01} = hc/\lambda_{ab}^{\max}$, where $\lambda_{ab}^{\max}$ is the main absorption peak; all parameters in CGS units [12]. Our calculations from the experimental absorption spectra show that all dyes have similar and large $\mu_{01} = 11 \div 13$ D, indicated as μ_{01}(exp) in Table 1.

Analysis of the fluorescence quantum yields for all PDs in the solvents of different polarity and viscosity (see Table 1), allows making the following conclusions:

1. In all solvents the smallest quantum yield is detected in PD AF, and the largest – in PD 3338. Asymmetrical PD 3294 shows an intermediate values. 2. Solvent polarity does not affect the fluorescence quantum yield for all dyes. 3. A strong increase in Φ_F is detected in glycerol: in ≈8 times for PD AF, ≈3 times for PD 3338, and ≈5 times for asymmetrical PD 3294. This viscosity-dependent effect is tentatively assigned to a restriction in possible rotation of the terminal residues around the bond connecting them with the chain, playing a major role in reducing fluorescence quantum yields in low-viscosity solvents. Thus, limitation of these rotations in glycerol results in a reducing of nonradiative internal conversion channel of S_1 energy deactivation.

Excitation anisotropy spectra for all compounds are performed in viscous GLY solutions to reduce rotational reorientation and at low concentrations (≈1 μM) to avoid reabsorption of the fluorescence. As known, the anisotropy value $r(\lambda)$ for a given excitation wavelength λ can be obtained as $r(\lambda) = \frac{I_{II}(\lambda)-I_{\perp}(\lambda)}{I_{II}(\lambda)+2I_{\perp}(\lambda)}$, where $I_{II}(\lambda)$ and $I_{\perp}(\lambda)$ are the intensities of the fluorescence signal (measured near the fluorescence maximum) polarized parallel and perpendicular to the excitation light, respectively [12]. Excitation anisotropy spectra, presented in Fig. 1, allow locating the spectral positions of the higher $S_0 \rightarrow S_n$ transitions, which cannot be easily distinguish from linear absorption measurements. As seen, the excitation anisotropy spectra reveal alternating peaks and valleys: the peaks indicate a small angle between the absorption and emission transition dipoles, while valleys indicate the larger angles between them. For all dyes anisotropy spectra are flat within the main $S_0 \rightarrow S_1$ absorption bands (up to ≈400 nm for PD AF, ≈450 nm for PD 3338 and ≈420 nm for PD 3294); $r(\lambda)$ values are high (≈0.36–0.38) indicating almost collinear alignment of the absorption and emission transition dipole moments. The decrease in the values of $r(\lambda)$ locates the position of the next electronic state (or group of states) with the larger angle between these two dipoles. The deepest valley is observed for PD 3338 in the range 380–420 nm indicating the angle up to 57° between them. Information gained from anisotropy measurements combined with quantum chemical calculations allows deeper understanding of the nature of electronic transitions.

Fluorescence decay curves for all dyes, measured by experimental setup shown in Fig. 2, are presented in Fig. 3. As seen, all curves show single-exponential character with the lifetimes of (100 ± 10) ps for PD AF, (270 ± 30) ps for PD 3338 and (180 ± 20) ps for asymmetrical PD 3294. Note that calculated and experimental lifetimes for all dyes agree within 10% error bar.

Quantum Chemical Analysis

Quantum chemical analysis is performed with the goal of understanding the formation of the linear absorption spectra in a series of the investigated dyes and their structure-property relations. Ground state geometry optimization is performed by DFT/6-31(d,p)/B3LYP method using the standard program package Gaussian 2003 [19]. The electronic transitions are

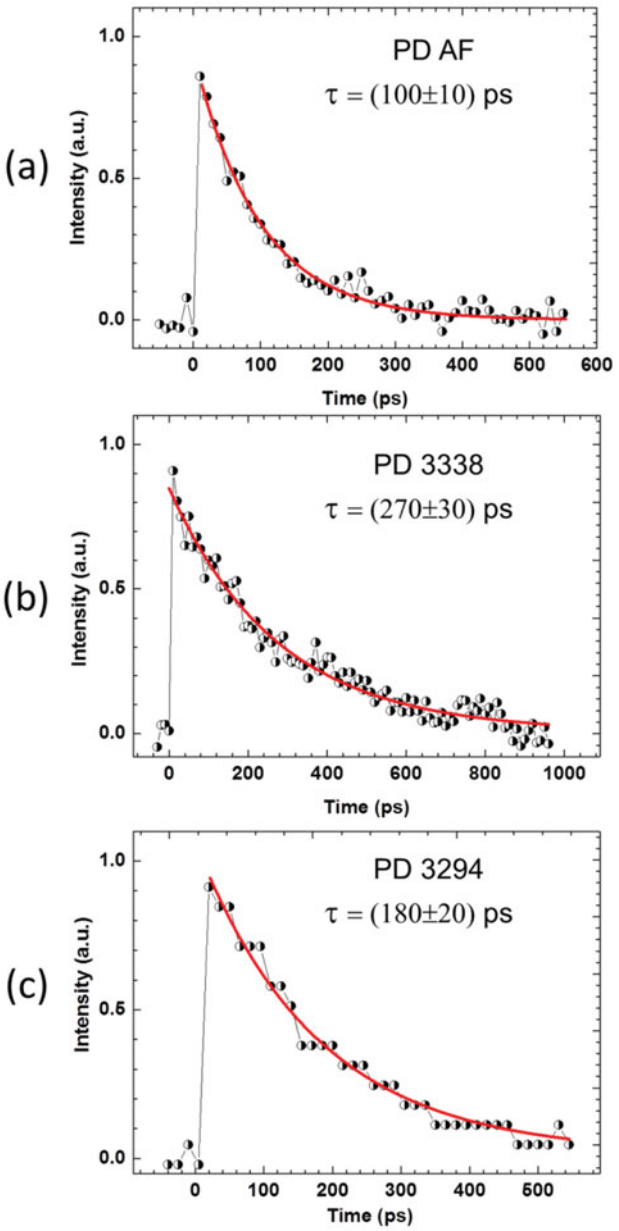

Figure 3. Fluorescence decay curves for PD AF (a), PD 3338 (b) and PD 3294 (c) in ACN.

calculated by semi-empirical ZINDO/S and, for comparison, by TD DFT methods. Both methods give a considerable divergence between the calculated and experimental absorption energies, which is known for PDs, especially absorbing in near IR region [20–21]. However, both methods give the same order of the molecular orbitals (MOs) and same charge distributions within them leading to the same order and same nature of the electronic transitions. Based on this information and performing a direct comparison calculated and

experimental data, we suppose to analyze correctly the nature of the electronic transitions in a homological series of dyes.

Ground State Geometry Optimization

The optimized molecular geometries for all investigated dyes in three dimensions are presented in Fig. 4. Our calculations show that the optimized molecular geometry for PD AF is planar without any spatial hindrances between the terminal groups. Only methyl groups in the terminal residues are positioned out of plane due to sp^3-hybridization of the corresponding carbon atoms. In PD 3338 polymethine chain is planar, however, benzoimidazole residues are rotated at 25° relative to the conjugated chain; benzoxazole groups are placed in the plane of the residues, while phenyl groups are rotated to 90°. In asymmetrical PD 3294 polymethine chain is also planar, and terminal groups are disposed accordingly to their symmetrical analogues, as shown in Fig. 4. Our quantum chemical calculations clearly show that only all trans-forms are the most energetically preferable in the ground state at the room temperature for all dyes as the energy barriers for formation of other types of isomers (including rotation around the bonds placed in the middle of the chain) are much larger than kT energy.

The calculated ground state charge distribution and carbon-carbon (CC) bond lengths alternation within polymethine chromophore are shown in Fig. 5. Note that all dyes contain

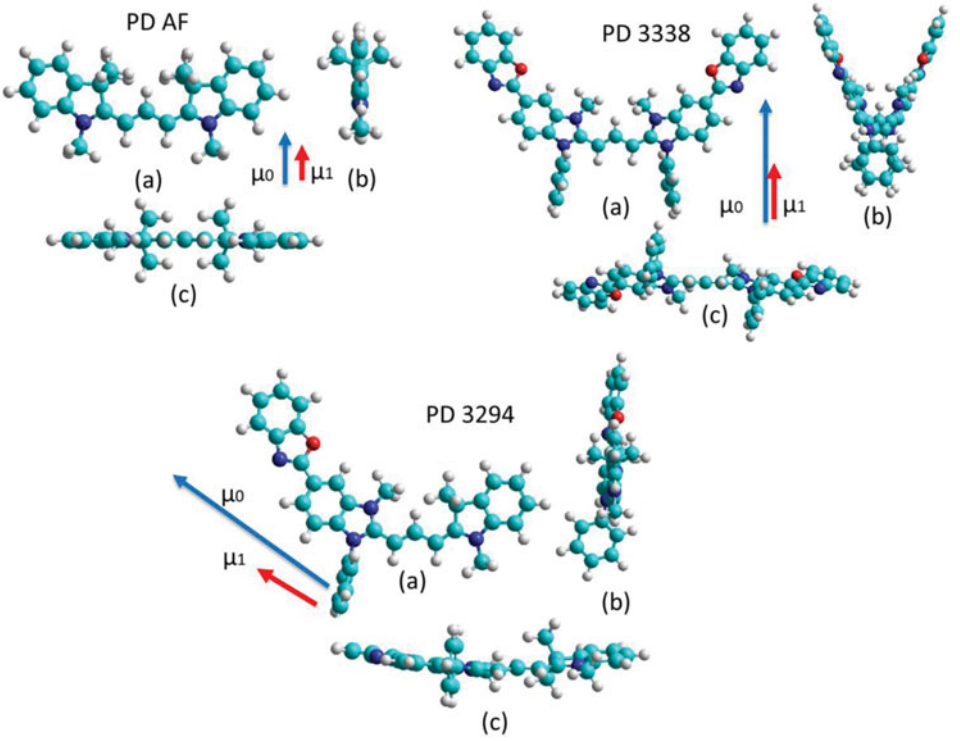

Figure 4. Optimized molecular geometries for all investigated dyes in three dimensions: (a) – XY (in plane); (b) –YZ; (c) – XZ. Arrows μ_0 and μ_1 illustrate the orientations of the permanent dipole moments in the ground and first excited states, correspondingly (values are shown in Table 1).

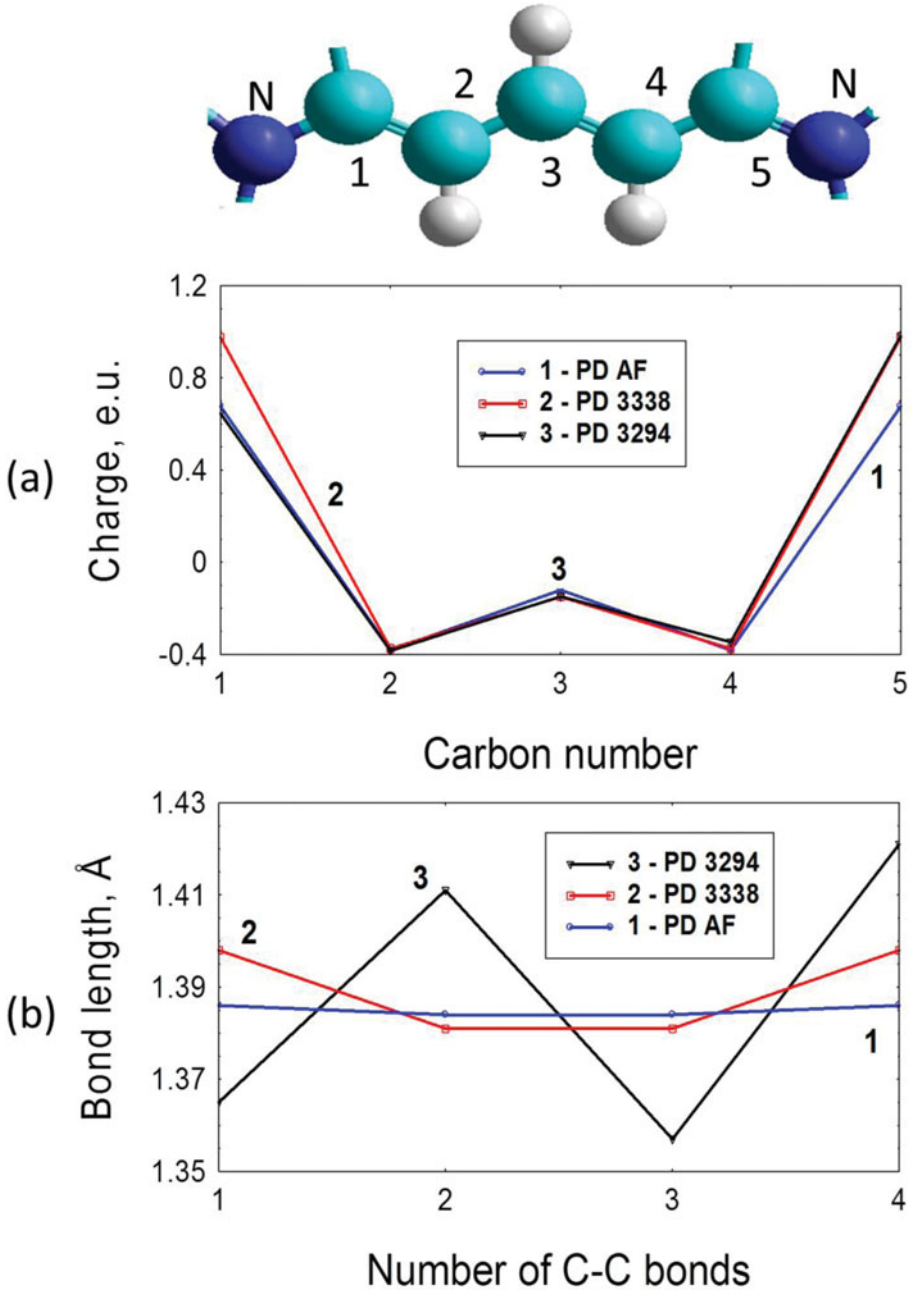

Figure 5. Charge distribution (a) and carbon-carbon bond length alternation (b) within polymethine chromophore for PD AF, PD 3338 and PD 3294.

the same polymethine chain, placed between two nitrogen atoms, as shown in Fig. 5. It is seen that the charge distribution for all dyes is identical within the chain and differ only nearby the terminal residues. Accordingly, for asymmetrical PD 3294 charge distributions close to terminal residues follow the trends of its symmetrical analogues.

The striking difference between symmetrical and asymmetrical dyes is observed for CC bond lengths behavior: bond lengths are almost equalized for symmetrical dyes, especially for PD AF, and equal to ≈1.39 Å which is typical CC bond length for polymethine chromophore, whereas they show strong alternation for asymmetrical PD 3294 as a result of different donor abilities in the terminal groups. Similar bond length alternation is typically observed for other asymmetrical polymethine dyes, where alternation is escalating from the terminal group with the higher donor ability to the terminal group with the smaller donor ability [22].

Electronic Transitions

Based on by DFT/6-31(d,p)/B3LYP optimized molecular geometries, the electronic transitions for a series of symmetrical-asymmetrical dyes were evaluated by coupling the semiempirical ZINDO Hamiltonian to a single configuration interaction scheme [23]. The active space involves the configurations generated by electron promotion from one of the highest occupied molecular orbitals (HOMOs) to one of the lowest unoccupied molecular orbitals (LUMOs) as implemented to a standard Gaussian package. Figure 6 schematically presents the positions and the shapes of the MOs involving into the formation of the electronic transitions in symmetrical-asymmetrical series of dyes with their main characteristics

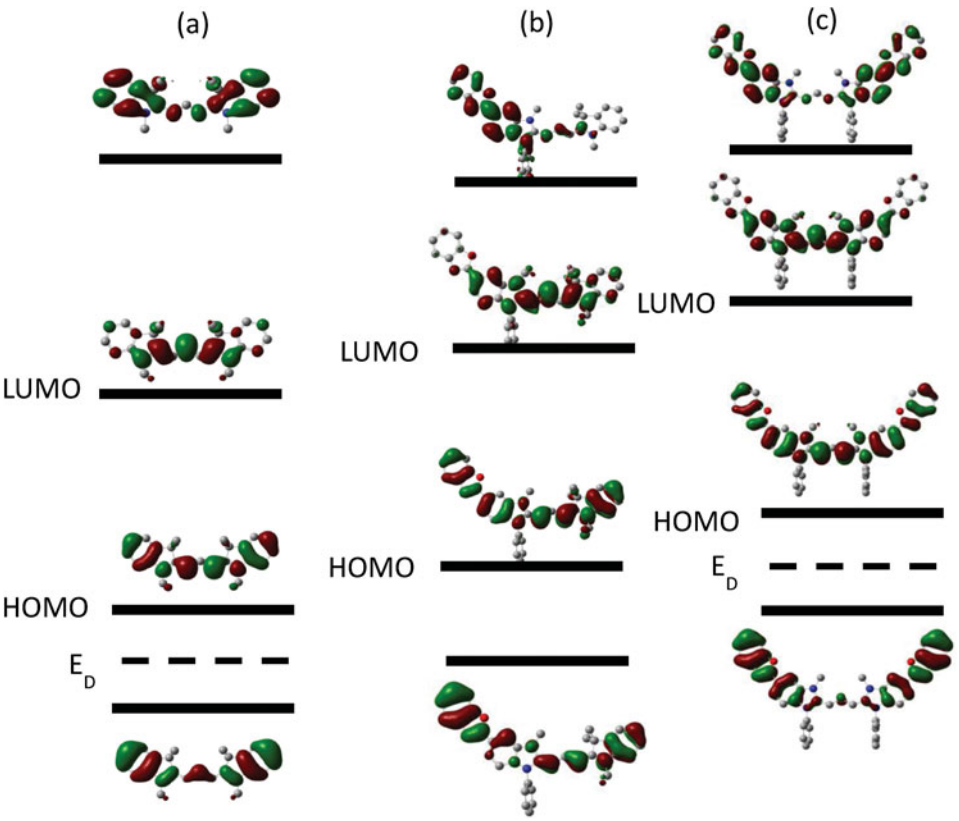

Figure 6. The shapes and schematic positions of the molecular orbitals for PD AF (a), PD 3338(b)and PD 3294 (c); E_D - middle position of the HOMO/HOMO-1 energy gap.

Table 2. Calculated characteristics of electronic transitions (ZINDO/S, OWF 0.4; CI 6 × 2)

Dye	Transitions	λ^{max}(abs), nm	f	μ_i	μ_{0i}	Main Configurations
	S_0			2.3		
PD AF	$S_0 \rightarrow S_1$	543	0.9	1.3	10.3	0.93 | HOMO→LUMO>
	$S_0 \rightarrow S_2$	415	0.02	3.3	1.3	0.95 | HOMO-1→LUMO>
	$S_0 \rightarrow S_3$	378	0.07	3.4	2.3	0.93 | HOMO-2→LUMO>
	$S_0 \rightarrow S_4$	367	0.01	4.0	1.03	0.96 | HOMO-3→LUMO>
	$S_0 \rightarrow S_5$	344	0.08	1.9	2.5	0.93 | HOMO-4→LUMO>
	$S_0 \rightarrow S_6$	280	0.06	1.2	1.9	0.92 | HOMO→LUMO+1>
	$S_0 \rightarrow S_7$	244	0.004	3.3	0.5	0.94 | HOMO-1→LUMO+1>
	S_0			5.0		
PD 3338	$S_0 \rightarrow S_1$	533	0.9	2.3	10.3	0.56 | HOMO→LUMO>-0.81 | HOMO-4→LUMO>
	$S_0 \rightarrow S_2$	400	0.04	20.4	1.7	0.97 | HOMO-1→LUMO>
	$S_0 \rightarrow S_3$	347	0.07	19.0	2.6	0.81 | HOMO→LUMO> +0.57 | HOMO-4→LUMO>
	$S_0 \rightarrow S_4$	345	0.001	30.2	0.3	0.78 | HOMO-2→LUMO> −0.64 | HOMO-3→LUMO>
	$S_0 \rightarrow S_5$	290	0.006	30.1	0.3	0.64 | HOMO-2→LUMO> −0.76 | HOMO-3→LUMO>
	$S_0 \rightarrow S_6$	288	0.001	28.7	4.9	0.85 | HOMO→LUMO+1>
	$S_0 \rightarrow S_7$	285	0.2	31.0	2.9	0.89 | HOMO-1→LUMO+1>
	S_0			10.8		
PD 3294	$S_0 \rightarrow S_1$	511	0.8	3.0	10.0	0.51 | HOMO→LUMO> +0.72 | HOMO-2→LUMO>
	$S_0 \rightarrow S_2$	387	0.1	13.5	3.4	0.68 | HOMO→LUMO> -0.65|HOMO-2→LUMO>
	$S_0 \rightarrow S_3$	360	0.2	12.1	4.3	0.90 | HOMO→LUMO+1>
	$S_0 \rightarrow S_4$	340	0.1	12.4	2.6	0.83 | HOMO-3→LUMO>
	$S_0 \rightarrow S_5$	325	0.008	25.3	0.8	0.85 | HOMO-4→LUMO>
	$S_0 \rightarrow S_6$	294	0.01	23.4	0.2	0.81 | HOMO-2→LUMO>
	$S_0 \rightarrow S_7$	266	0.04	21.4	1.6	0.90 | HOMO-1→LUMO+1>

Notes. λ^{max}(abs) - wavelengths of the absorption peaks; f - oscillator strength; μ_i – permanent dipole moments of the S_i state; μ_{0i} – $S_0 \rightarrow S_i$ transition dipole moment.

listed in Table 2. The first electronic transitions $S_0 \rightarrow S_1$ for all dyes are typical allowed "cyanine-like" transitions with the large oscillator strengths (f = 0.8–0.9) corresponding to transition dipole moments μ_{01} = 10–10.3 D, while all other $S_0 \rightarrow S_n$ transitions are characterized by very small oscillator strengths and transition dipole moments, in agreement with the experimental data presented in Table 1. Important to note that all transitions for PD AF are "pure," corresponding to electron promotion from a single HOMO to a single

LUMO, whereas most of the transitions for PD 3338 are mixed due to existence of the own π-conjugated system within terminal groups. Correspondingly, for asymmetrical PD 3294 at least two lowest electronic transitions are also mixed as they involve MOs located within benzoimidazole terminal groups.

It is established earlier that the donor terminal groups containing own π-conjugated system can significantly affect the positions and charge distribution of the highest occupied orbitals in D–π–D symmetrical polymethine molecules [24]. These HOMOs in each dye molecule, which we call *donor orbitals*, are formed by the mixing, interaction and splitting of the HOMOs of two identical terminal residues and HOMO of the conjugated chain. For PD AF and PD 3338 *donor orbitals* are HOMO (with the asymmetrical charge distribution) and HOMO-1 (with the symmetrical charge distribution). Note that the energy positions of the *donor orbitals* are determined by the donor strength of corresponding terminal residues, therefore, a middle position of the HOMO/HOMO-1 energy gap (indicated as E_D in Fig. 6) may be proposed for the qualitative characterization of the donor ability/strength for the corresponding symmetrical dye. It is clearly seen from Fig. 6 that the donor strength of PD 3338 is much more that for PD AF. Lowest unoccupied molecular orbital, LUMO, in PD AF represents a level of the charge and originates mainly from LUMO of the polymethine chain, which is typical for all cationic dyes [24]. For symmetrical PD 3338, charge within LUMO is more delocalized extending from the chain to the terminal groups. As a result, HOMO-LUMO gap increases leading to a blue shift of the absorption spectrum.

Thus, performed investigations have advanced our understanding of the nature of the electronic transitions and the structure–property relations in a series of symmetrical-asymmetrical polymethine molecules, which is important for understanding of the linear and nonlinear optical behavior of these dyes and associated optical applications.

Conclusions

In summary, we performed a detailed experimental investigation of the steady-state and time-resolved spectral properties of new cationic asymmetrical trimethine cyanine dye with indolenine and benzoimidazole terminal groups of different donor abilities in comparison with its symmetrical analogues.

1. Steady-state spectral-luminescence measurements revealed close to mirror-symmetric absorption and fluorescence shapes with the small Stokes for the symmetrical dyes, while the fluorescence spectrum of new asymmetrical dye is twice more narrow than the absorption bandwidth and is similar to that of symmetrical PDs (independently of solvent polarity and viscosity) in agreement with the results obtained earlier for other asymmetrical PDs. A strong increase in the fluorescence quantum yield is detected in viscous glycerol: in $\approx$8 times for PD AF, $\approx$3 times for PD 3338, and $\approx$5 times for asymmetrical PD 3294. This viscosity-dependent effect is assigned to a restriction in possible rotation of the terminal residues around the bond connecting them with the chain, playing a major role in nonradiative internal conversion channel of S_1 energy deactivation. This effect can be successfully used for probing the viscosity of the microenvironments in biomolecules and polymeric materials.
2. Kerr-gated time-resolved study of the fluorescence properties of the investigated molecules has been performed using femtosecond laser system. All decay curves show single-exponential character with the lifetimes of (100 $\pm$ 10) ps for PD AF,

(270 ± 30) ps for PD 3338 and (180 ± 20) ps for asymmetrical PD 3294 in agreement with the calculated values.

3. Quantum chemical analysis, performed with the goal of understanding the formation of the linear absorption spectra in the investigated series, allowed to determine the charge distribution, bond length alternation, permanent and transition dipole moments and the positions and the shapes of the molecular orbitals involved into the formation of the $S_0 \rightarrow S_n$ electronic transitions. All results fully agree with the spectral-luminescence investigations, especially excitation anisotropy studies allowing to locate the spectral positions of the higher electronic transitions, which cannot be distinguish from the linear absorption measurements.

Obtained results might provide a foundation for the future design of new cyanine fluorophores for multifunctional chemical, biological and optical applications.

Acknowledgments

The authors thank the employees of the NASU Center for collective use of "Laser femtosecond complex" and personally prof. I. M. Dmytruk for help in carrying out the time-resolved experiment. This work is supported by the National Academy of Sciences of Ukraine (grants 1.4.1.B/153 and VC/157).

References

[1] Mishra, A., Behera, R. K., Behera, P. K., Mishra, B. K., & Behera, G. B. (2000). *A Review. Chem. Rev.*, *100*, 1973.
[2] Fabian, J., Nakazumi, H., & Matsuoka, M. (1992). *Chem. Rev.*, *92*, 1197.
[3] Marder, S. R. (2006). *Chem. Commun.*, 131.
[4] Peyghambarian, N., Dalton, L., Kippelen, B., Marder, S., Norwood, R., & Perry, J. (2006). *Laser Focus World*, *42*, 85.
[5] Daehne, S. (1978). *Science*. *199*, 1163.
[6] Przhonska, O.V. et. al. (2010). In: *Advanced Fluorescence Reporters in Chemistry and Biology I: Fundamentals and Molecular Design*, Demchenko, A.P. (Ed.), Chapter 4, Springer-Verlag Berlin: Heidelberg, 105.
[7] Hamer, F. M. (1964). *The Cyanine Dyes and Related Compounds*, Interscience Publishers: New York, USA.
[8] Fu, J., Lazaro, A., Padilha, L. A., Hagan, D. J., Van Stryland, E. W., Przhonska, O. V., Bondar, M. V., Slominsky, Yu. L., & Kachkovski, A. D. (2007). *J. Opt. Soc. Am. B*, *24*, 67.
[9] Zubarovskii, V. M., Moskaleva, R. N., & Bachurina, M. P. (1964). *Ukr. Chim. Zhurn.*, *30*, 80.
[10] Zubarovskii, V. M., & Khodot, G. P. (1977). *Ukr. Chim. Zhurn.*, *43*, 381.
[11] Kubin, R. F., & Fletcher, A. N. (1982). *J. Lumin.*, *27*, 455.
[12] Lakowicz, J. R. (1999). *Principles of Fluorescence Spectroscopy*, Kluwer: New York, USA.
[13] Beddard, G. (1993). *Rep. Prog. Phys.*, *56*, 63.
[14] Takeda, J., Nakajima, K., Kurita, S., Tomimoto, S., Saito, S., & Suemoto, T. (2000). *Phys. Rew. B.*, *62*, 10083.
[15] Sajadi, M., Dobryakov, A. L., Garbin, E., Ernsting, N. P., & Kovalenko, S. A. (2010) *Chem. Phys. Lett.*, *489*, 44.
[16] Symes, D. R., Wegner, U., Ahlswede, H.-C., Streeter, M. J. V., Gallegos, P. L., Divall, E. J., Smith, R. A., Rajeev, P. P. & Neely D. (2010). *Appl. Phys .Lett.*, *96*, 011109.
[17] Ischenko, A. A., Derevyanko, N. A., & Sridro, V. A. (1999). *Dyes Pigments*, *19*, 169.
[18] Strickler, S. J. & Berg, R. A. (1962). *J. Chem. Phys.*, *37*, 814.

[19] Frisch, M. J. et. al. (2003) *Gaussian 03, revision B.05*, Gaussian, Inc.: Pittsburgh, PA.
[20] Fabian, J. & Hartmann, H.(2008). *Dyes Pigments*, *79*, 126.
[21] Fabian, J. (2010). *Dyes Pigments*, *84*, 36.
[22] Kachkovsky, A. D. (1997). *Russ. Chem. Rev.*, *66*, 715.
[23] Tomlinson, A., & Yaron, D. (2003). *J. Comput. Chem.*, *24*, 1782.
[24] Webster, S., Fu, J., Padilha, L. A., Przhonska, O. V., Hagan, D. J., Van Stryland, E. W., Bondar, M. V., Slominsky, Yu. L., & Kachkovski, A. D. (2008). *Chem. Phys.*, *348*, 143.